Available online at www.sciencedirect.com
ScienceDirect
International Journal of Thermal Sciences 48 (2009) 290–302
International Journal of Thermal Sciences
www.elsevier.com/locate/ijts

Numerical study of turbulent flow and heat transfer characteristics of nanofluids considering variable properties

Praveen K. Namburu, Debendra K. Das *, Krishna M. Tanguturi, Ravikanth S. Vajjha

Department of Mechanical Engineering, University of Alaska, Fairbanks, P.O. Box 755905, Fairbanks, AK 99775-5905, USA

Received 29 July 2007; received in revised form 19 December 2007; accepted 3 January 2008

Available online 5 February 2008

Abstract

Turbulent flow and heat transfer of three different nanofluids (CuO, Al_2O_3 and SiO_2) in an ethylene glycol and water mixture flowing through a circular tube under constant heat flux condition have been numerically analyzed. New correlations for viscosity up to 10% volume concentration for these nanofluids as a function of volume concentration and temperature are developed from the experiments and are summarized in the present paper. In our numerical study, all the thermophysical properties of nanofluids are temperature dependent. Computed results are validated with existing well established correlations. Nusselt number prediction for nanofluids agrees well with Gnielinski correlation. It is found that nanofluids containing smaller diameter nanoparticles have higher viscosity and Nusselt number. Comparison of convective heat transfer coefficient of CuO, Al_2O_3 and SiO_2 nanofluids have been presented. At a constant Reynolds number, Nusselt number increases by 35% for 6% CuO nanofluids over the base fluid.

Keywords: Nanofluid; Nanoparticles; Viscosity; Turbulent flow; Heat transfer enhancement; Convection

1. Introduction

Nanofluids are created by dispersing nanometer-sized particles (< 100 nm) in a base fluid such as water, ethylene glycol or propylene glycol. Use of high thermal conductivity metallic nanoparticles (e.g., copper, aluminum, silver and silicon) increases the thermal conductivity of such mixtures, thus enhancing their overall energy transport capability [27]. Nanofluids have attracted attention as a new generation of heat transfer fluids in building heating, in heat exchangers, in plants and in automotive cooling applications, because of their excellent thermal performance. Various benefits of the application of nanofluids include: improved heat transfer, heat transfer system size reduction, minimal clogging, microchannel cooling and miniaturization of systems [7]. Therefore, research is underway to apply nanofluids in environments where higher heat flux is encountered and the conventional fluid is not capable of achieving the desired heat transfer rate.

A great deal of energy is expended heating residential and industrial buildings in the cold regions of the world. Due to the severe winter conditions, ethylene glycol or propylene glycol mixed with water in different volume percentages are typically used to lower the aqueous freezing point of the heat transfer medium [20]. Such heat transfer fluids are used in heat exchangers, baseboard heaters in homes, automobiles and in industrial plants in cold regions. These fluids can withstand low temperatures down to $-60\,^{\circ}C$. At low temperatures, ethylene glycol mixtures have better heat transfer characteristics than propylene glycol mixtures [2]. A 60% ethylene glycol and 40% water by weight fluid mixture is most commonly used in the sub-arctic and arctic regions of Alaska.

In order to evaluate the superior heat transfer characteristics of nanofluids there must be ample data on the thermophysical properties of such fluids. Eastman et al. [10] observed that with 0.3% volume concentration of copper nanoparticles dispersed in ethylene glycol, its thermal conductivity increased by 40%. Das et al. [8] have reported a 10–25% increase in thermal conductivity with 1–4% volume concentration of alumina nanoparticles in water. Kulkarni et al. [16] reported that the experimental viscosity values of Copper oxide (CuO) dispersed in

* Corresponding author. Tel.: +1 907 474 6094; fax: +1 907 474 6141.
E-mail address: ffdkd@uaf.edu (D.K. Das).

1290-0729/$ – see front matter
doi:10.1016/j.ijthermalsci.2008.01.001

Nomenclature

x	Distance from the inlet	m	
L	Length of the tube	m	
D	Diameter of the tube	m	
T	Temperature	K	
q''	Heat flux	W/m^2	
V	Velocity	m/sec	
c	Specific heat	J/kg K	
k	Thermal conductivity	W/m K	
h	Heat transfer coefficient, $(h = q''/T_w - T_{bm})$	W/m^2 K	
Nu	Nusselt number, $Nu = (hD/K)$		
Re	Reynolds number, $Re = (\rho V D/\mu)$		
Pr	Prandtl number, $Pr = (\mu c/k)$		
f	Friction factor		
C_f	Skin friction coefficient		

Greek letters

ϕ	Volume concentration	%
ρ	Density	kg/m^3
μ	Viscosity	mPa s

Subscripts

p	Nanoparticle
nf	Nanofluid
bf	Base fluid
in	Inlet
out	Outlet
w	Wall
bm	Bulk mean

propylene glycol and water mixture are much higher than those predicted by Batchelor [3] equation. A review article by Wang and Mujumdar [28] lists studies conducted on the thermal conductivity and heat transfer of various nanofluids. However, no universal correlations have been developed thus far to calculate the properties of all types of nanofluids of all concentrations.

Pak and Cho [24] performed viscosity, pressure loss and heat transfer measurements on titanium dioxide nanofluids up to 3% concentration by volume and found single-phase correlations can be successfully extended to nanofluids. They reported increase in the convective heat transfer coefficient with particle volume concentration and Reynolds number. They also reported Nusselt numbers increased by 30% over the Dittus–Boelter [9] equation for single phase fluids. A new correlation for the turbulent convective heat transfer for dilute concentration of nanofluids was proposed by them.

$$Nu = 0.021 Re^{0.8} Pr^{0.5}$$
$$\text{for } 6.54 \leqslant Pr \leqslant 12.33; \qquad 10^4 \leqslant Re \leqslant 10^5 \tag{1}$$

Xuan and Li [27] performed experimental study on Cu–water nanofluids up to 2% volume concentration and developed a Nusselt number correlation. They found that Cu–water dilute nanofluids have almost same pressure drop as water under the same Reynolds number. Heris et al. [14] performed laminar convective heat transfer experiments on CuO/water and aluminum oxide (Al_2O_3)/water nanofluids and concluded that the heat transfer enhancement by nanofluids depends on several factors including increment of thermal conductivity, nanoparticle type, size, base fluid, flow regime and the boundary conditions. Nguyen et al. [23] experimentally investigated the heat transfer characteristics of Al_2O_3/water nanofluids for an electronic cooling application. They found the heat transfer coefficient with 6.8% particle volume concentration increased as much as 40% compared to the base fluid.

Maiga et al. [18] conducted a numerical study on γ–Al_2O_3 nanofluids flow under forced laminar convection in circular tubes and between parallel disks. For a range of Reynolds number from 250 to 1000 they concluded that the heat transfer enhancement is much more pronounced with the increase in particle concentration. However, they observed a drastic adverse effect on wall shear stress in comparison to the base fluid. For the analysis of flow between discs, they found insignificant effect on heat transfer with the variation of gap between the discs. Akbarinia and Behzadmehr [1] presented a numerical study of nanofluids under mixed laminar convection in a curved tube. They compared the variations of Nusselt number with Grashof number for various volume percentages of Al_2O_3 nanoparticles in water. They found that at large Grashof number the skin friction was reduced. A second study by Maiga et al. [19] presented the numerical study of hydrodynamic and thermal behaviors of fully developed turbulent flow of Al_2O_3/water nanofluids inside a circular tube subjected to a uniform heat flux of 50 W/cm^2. A new correlation for Nusselt number was derived from their study.

$$Nu = 0.085 Re^{0.71} Pr^{0.35}$$
$$\text{for } 6.6 \leqslant Pr \leqslant 13.9; \qquad 10^4 \leqslant Re \leqslant 5 \times 10^5 \tag{2}$$

Ethylene glycol and water (EG/water) based nanofluids are required for application in cold regions, which have not been studied widely thus far. Since the sub-zero temperature operation needed the rheological properties, viscosity measurements of various nanofluids have been investigated. New viscosity correlations as a function of temperature and volume concentration for Silicon dioxide (SiO_2) and Al_2O_3 nanoparticles in EG/water (60:40 by mass) base fluid have been presented. The present paper covers the rheological investigations of nanofluids up to 10% volume concentration and heat transfer computation up to 6%. Using the rheological properties we have presented numerical computations for turbulent forced convection, which will be useful in the design of heat transfer systems in cold climates. Comparisons of the computed Nusselt number with the correlations developed by Pak and Cho [24] and Maiga et al. [19] have been presented. Furthermore, the previous investigations were limited to dilute concentration up to 3%. In the present study the Prandtl number are in much higher range $47 \leqslant Pr \leqslant 105$ than those reported by the earlier researchers.

2. Thermophysical properties of nanofluids

Thermophysical properties of nanofluids are calculated by using the formulas summarized by Buongiorno [6].

$$\rho_{nf} = \phi\rho_p + (1-\phi)\rho_{bf} \tag{3}$$

It should be noted that for calculating the specific heat of nanofluid some of prior researchers have used the following correlation

$$c_{nf} = \phi c_p + (1-\phi)c_{bf} \tag{4}$$

It is modified in our analysis to Eq. (5) presented by Buongiorno [6] which is more accurate.

$$c_{nf} = \frac{\phi\rho_p c_p + (1-\phi)\rho_{bf}c_{bf}}{\rho_{nf}} \tag{5}$$

The most commonly used thermal conductivity equation (6) was proposed by Hamilton and Crosser [13] for the mixtures containing micrometer size particles; it is assumed that this equation is applicable for the nanofluids.

$$\frac{k_{nf}}{k_{bf}} = \frac{k_p + (n-1)k_{bf} - (n-1)\phi(k_{bf}-k_p)}{k_p + (n-1)k_{bf} + \phi(k_{bf}-k_p)} \tag{6}$$

In the above equation n is the shape factor and is equal to 3 for spherical nanoparticles. Zhang et al. [30] have shown that this correlation accurately predicts the thermal conductivity of nanofluids.

The properties of base fluid, EG/water at different temperatures ($\geqslant$ 293 K) are available in ASHRAE [2]. These properties as a function of temperature were curve fitted from ASHRAE data. Then they were substituted in the density, specific heat, thermal conductivity equations (3), (5) and (6) to evaluate the properties of nanofluids at different temperatures and concentrations. Therefore, in our simulations the properties of nanofluids are temperature dependent. The properties of solid particles are taken to be constant in the present operating range of 293 K to about 363 K, the highest encountered temperature near the wall that occurs at a Reynolds number of 10^4.

2.1. Viscosity of nanofluids

The experimental setup and the procedure to measure the viscosity are described by Kulkarni et al. [15]. First, the viscometer [5] was calibrated using Brookfield's Silicone Viscosity Standard fluids (viscosity values of 9.7 and 97 m Pa s at 25 °C). The equipment accuracy was found to be within ±2% of these standard viscosity values. The apparatus was further tested with viscosity measurements of 60:40 EG/water solution. The obtained readings were compared with the data from the ASHRAE Handbook [2] and the experimental values matched closely with a maximum difference of ±2%.

Viscosity of CuO and EG/water nanofluids with particle diameter of 29 nm with volume concentration 1–6% is calculated from the correlation developed by Namburu et al. [21].

$$\mathrm{Log}\,\mu_{nf} = Ae^{-BT} \tag{7}$$

where T is the temperature in Kelvin, and ranging from 238 K (−35 °C) to 323 K (50 °C) and A and B are functions of volumetric concentration ϕ. The factors A and B are given by

$$A = 1.8375(\phi)^2 - 29.643(\phi) + 165.56 \quad \text{with } R^2 = 0.9873 \tag{8}$$

$$B = 4\times10^{-6}(\phi)^2 - 0.001(\phi) + 0.0186 \quad \text{with } R^2 = 0.9881 \tag{9}$$

In the above expressions ϕ ranges from 0 to 6.12.

Viscosity values of Al_2O_3 and EG/water nanofluids (53 nm) were measured for 1–10% volume concentrations. From the experimental data a correlation was developed that related nanofluid viscosity with particle volume concentration and the temperature of the nanofluid, similar to Eq. (7). Here T is the temperature in Kelvin in the same range as in Eq. (7) and A and B are functions of volumetric concentration ϕ, which are given by

$$A = -0.29956(\phi)^3 + 6.7388(\phi)^2 - 55.444(\phi) + 236.11 \quad \text{with } R^2 = 0.9978 \tag{10}$$

$$B = (-6.4745(\phi)^3 + 140.03(\phi)^2 - 1478.5(\phi) + 20341)/10^6 \quad \text{with } R^2 = 0.9994 \tag{11}$$

In the above expressions, ϕ ranges from 1 to 10.

Viscosity values of SiO_2 and EG/water nanofluids (20, 50 and 100 nm) were measured for 2–10% volume concentrations. From the experimental viscosity values, a correlation for 50 nm SiO_2 nanofluids was developed similar to Eq. (7) that related nanofluid viscosity with particle volume concentration and the temperature of the nanofluid [22]. Here T is the temperature in Kelvin in the same range as Eq. (7) and A and B are functions of volumetric concentration ϕ, which are given by

$$A = 0.1193(\phi)^3 - 1.9289(\phi)^2 - 2.245(\phi) + 167.17 \quad \text{with } R^2 = 0.981 \tag{12}$$

$$B = -7\times10^{-6}(\phi)^2 - 0.0004(\phi) + 0.0192 \quad \text{with } R^2 = 0.99 \tag{13}$$

In the above expressions, ϕ ranges from 2 to 10.

An effort to combine the viscosity correlations of three nanofluids to a single equation was not successful.

2.2. Particle diameter effect on the viscosity of nanofluids

From our experiments on the viscosity of SiO_2 nanofluids of different particle diameters 20, 50 and 100 nm exhibited in Fig. 1, we observed that the nanoparticles of smaller diameter posses the higher viscosity for the same volume concentration of nanofluids. This is physically quite realistic because for a given volume concentration, smaller diameter nanoparticles will be more in number and the total surface area of these smaller diameter nanoparticles will be more. Therefore, smaller diameter nanoparticles interact with the surrounding fluid over a greater surface area, thus increasing the viscosity.

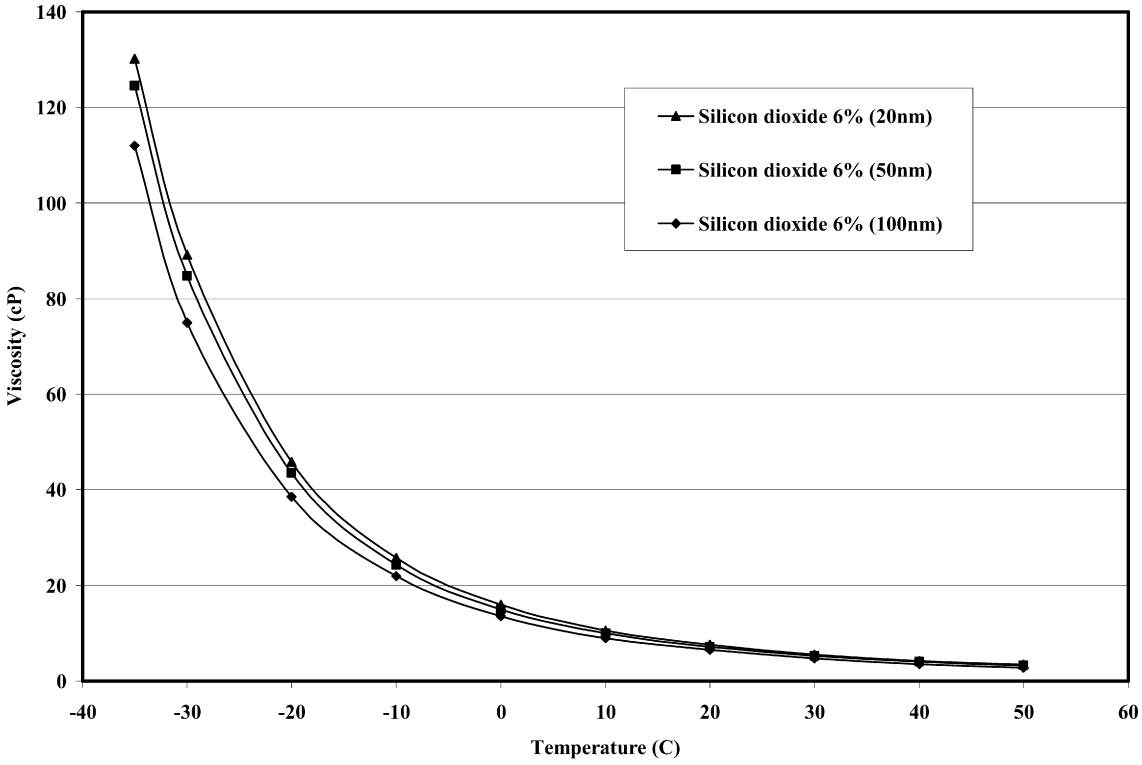

Fig. 1. Effect of nanoparticles diameter on the viscosity of SiO_2 nanofluids with 6% volume concentration.

Table 1
Thermophysical properties of the nanofluids used in the numerical computations at inlet temperature of 293 K

Type of fluid	Volume concentration (%)	Viscosity (mPa s)	Density (kg/m^3)	Specific heat (J/kg K)	Thermal conductivity (W/m K)	Prandtl number
EG/water (base fluid)	0	5.38	1086.27	3084.00	0.349	47.54
CuO/EG water	1	6.15	1138.51	2942.61	0.359	50.40
CuO/EG water	2	6.83	1190.74	2813.63	0.369	52.04
CuO/EG water	3	9.08	1242.98	2695.50	0.380	64.46
CuO/EG water	4	11.38	1295.22	2586.89	0.390	75.42
CuO/EG water	5	14.00	1347.46	2486.70	0.401	86.78
CuO/EG water	6	18.75	1399.69	2393.99	0.424	105.82
SiO_2/EG water (20 nm)	6	7.58	1154.29	2814.09	0.381	55.97
SiO_2/EG water (50 nm)	6	7.16	1154.29	2814.09	0.381	52.87
SiO_2/EG water (100 nm)	6	6.53	1154.29	2814.09	0.381	48.22
Al_2O_3/EG water	6	9.67	1259.29	2645.35	0.425	60.23

This is an interesting result regarding the influence of nanoparticle size on viscosity of nanofluids and believed to be reported for the first time. We measured viscosity of SiO_2 nanofluid with three particle diameters. However, this data was not sufficient to develop a correlation of viscosity as a function of particle diameter. This should be an important area of research in the future.

2.3. Table of thermophysical properties used in computations

All the thermophysical properties discussed above were incorporated in the present numerical analysis to compute the turbulent heat transfer for three different types of nanofluids which are summarized in Table 1. The viscosity values are measured values and the other properties are calculated from theoretical correlations. The influence of viscosity is more profound on pumping power and heat transfer in comparison with other thermophysical properties of nanofluids. Viscosity is a strong function of temperature and the theoretical correlations available are off from the measured values. Therefore we developed new correlations for viscosities from our experiments. As an example, the inclusion of properties variations in our computational analysis is illustrated in Table 1 for one temperature.

Notice the dominant change of viscosity with concentration. The Prandtl number which greatly influences heat transfer is also varying over a large range for the three nanofluids shown.

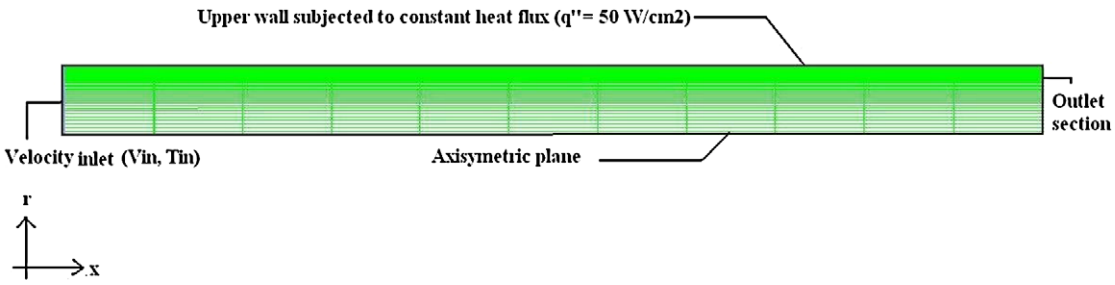

Fig. 2. Grid layout used in the present analysis, axisymmetric about X-axis.

3. Mathematical modeling

3.1. Assumptions

The nanoparticles in the base fluid may be easily fluidized and consequently the effective mixture behaves like a single phase fluid [27]. It is also assumed that the fluid phase and nanoparticles are in thermal equilibrium with zero relative velocity. This may be realistic as nanoparticles are much smaller than microparticles and the relative velocity decreases as the particle size decreases. The resultant mixture may be considered as a conventional single phase fluid. The thermal and physical properties are temperature dependent under the operating conditions. The effective thermophysical properties are dependent upon the temperature and volume concentration. Furthermore the assumption of single phase for a nanofluid is validated to an extent through the experimental results of Pak and Cho [24] and Xuan and Li [27]. Under these assumptions, the classical theory of single phase fluid can be applied to nanofluids.

3.2. Governing equations

The problem under investigation is a two-dimensional (axisymmetric) steady, forced turbulent convection flow of nanofluid flowing inside a straight circular tube having diameter of 0.01 m and a length of 0.8 m. The fluid enters the circular tube with uniform axial velocity and temperature. The flow and thermal fields are assumed to be axisymetric with respect to the horizontal plane parallel to X-axis as shown in Fig. 2.

The governing equations for the fluid flow are [26]:

$$\operatorname{div}(\rho \bar{V}) = 0 \tag{14}$$

$$\operatorname{div}(\rho \bar{V} \bar{V}) = -\operatorname{grad}(\bar{P}) + \mu \nabla^2 \bar{V} - \operatorname{div}(\rho \overline{u'u'}) \tag{15}$$

$$\operatorname{div}(\rho \bar{V} c_p \bar{T}) = \operatorname{div}(k \operatorname{grad} \bar{T} - \rho c_p \overline{u't'}) \tag{16}$$

In the above equations, the symbols $\bar{V}$, $\bar{P}$ and $\bar{T}$ represent the time averaged flow variables, while the symbols u' and t' represent the fluctuations in velocity and temperature. The terms in the governing equations $\rho \overline{u'u'}$ and $\rho c_p \overline{u't'}$ represent the turbulent shear stress and turbulent heat flux. These terms are unknown and must be approximately expressed in terms of mean velocity and temperature.

3.3. Turbulence modeling

For closure of the governing equations of fluid flow, empirical data or approximate models are required to express the turbulent stresses and heat flux quantities of the related physical phenomenon. In the present numerical analysis, κ–ε turbulent model proposed by Launder and Spalding [17] was adopted. κ–ε turbulent model introduces two additional equations namely turbulent kinetic energy (κ) and rate of dissipation (ε).

The equations for turbulent kinetic energy (κ) and rate of dissipation (ε) are given by;

$$\operatorname{div}(\rho \bar{V} \kappa) = \operatorname{div}\left\{(\mu + \mu_t)/\sigma_\kappa \operatorname{grad} \kappa\right\} + G_\kappa - \rho\varepsilon \tag{17}$$

$$\operatorname{div}(\rho \bar{V} \varepsilon) = \operatorname{div}\left\{\left(\mu + (\mu_t/\sigma_\varepsilon)\right) \operatorname{grad} \varepsilon\right\} + C_{1\varepsilon}(\varepsilon/\kappa) G_\kappa + C_{2\varepsilon} \rho (\varepsilon^2/\kappa) \tag{18}$$

In the above equations, G_κ represents the generation of turbulent kinetic energy due to mean velocity gradients, σ_κ and σ_ε are effective Prandtl numbers for turbulent kinetic energy and rate of dissipation, respectively; $C_{1\varepsilon}$ and $C_{2\varepsilon}$ are constants and μ_t is the eddy viscosity and is modeled as

$$\mu_t = (\rho C_\mu \kappa^2)/\varepsilon \tag{19}$$

C_μ is a constant and its value is 0.09.

In Eqs. (17) and (18); $C_{1\varepsilon} = 1.44$; $C_{2\varepsilon} = 1.92$; $\sigma_\kappa = 1.0$ and $\sigma_\varepsilon = 1.3$.

Further information is available in Launder and Spalding [17] and Fluent [11] for turbulence modeling.

3.4. Boundary conditions

The governing equations of the fluid flow are non-linear and coupled partial differential equations, subjected to the following boundary conditions. At the tube inlet section, uniform axial velocity V_{in}, temperature T_{in}, turbulent intensity and hydraulic diameter [11] have been specified. At the outlet section, the flow and temperature fields are assumed fully developed ($(x/D) > 10$). Outflow boundary condition has been implemented for the outlet section. This boundary condition implies zero normal gradients for all flow variables except pressure. Only half of the tube was modeled due to the symmetry. On the upper wall of the tube, the no-slip boundary condition was imposed. The wall is subjected to a uniform heat flux. On the lower wall of the modeled domain, the axis boundary condition was applied. In the present analysis, the near wall treatment was based on enhanced wall functions [11].

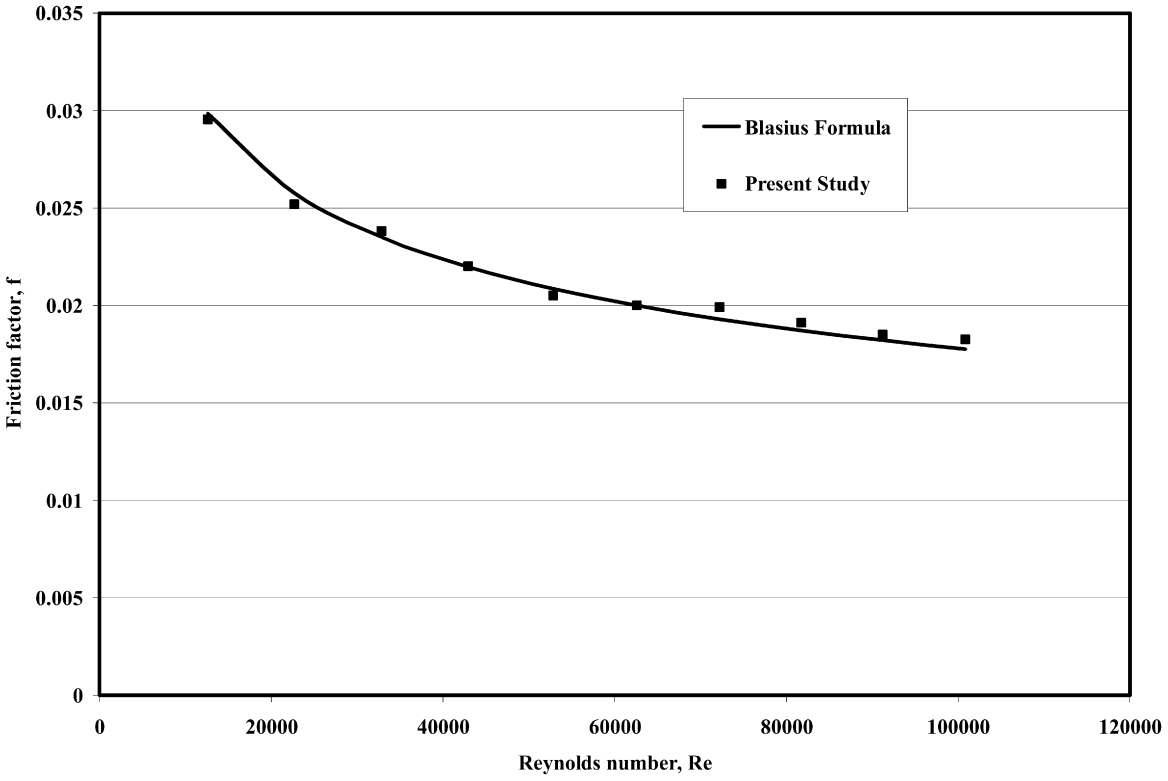

Fig. 3. Comparison of Darcy friction factor by Blasius formula and computed values for EG/water in turbulent regime.

3.5. Numerical method

The computational fluid dynamics code Fluent was used for solving this problem. The system of governing equations (14)–(18) were solved by control volume approach. Control-volume technique converts the governing equations to a set of algebraic equations that can be solved numerically. The control volume approach employs the conservation statement or physical law represented by the entire governing equations over finite control volumes. First order upwind scheme was employed to discretize the convection terms, diffusion terms and other quantities resulting from governing equations. Grid schemes used are staggered in which velocity components are evaluated at the center of control volume interfaces and all scalar quantities are evaluated in the center of control volume. Pressure and velocity were coupled using Semi Implicit Method for Pressure Linked Equations [SIMPLE] [25]. Fluent solves the linear systems resulting from discretization schemes using a point implicit (Gauss–Seidel) linear equation solver in conjunction with an algebraic multigrid method. During the iterative process, the residuals were carefully monitored. For all simulations performed in the present study, converged solutions were considered when the residuals resulting from iterative process for all governing equations (14)–(18) were lower than 10^{-6}.

3.6. Grid optimization

The grid used in the present analysis was 100×150, 100 in r-direction and 150 in x-direction. We also tested 150×200 and 200×250. All gave similar values of velocity and temperature at the outlet. Therefore, 100×150 was accepted as the optimal grid size. This grid size was validated by our CFD results in Figs. 3 and 4.

4. Results and discussions

4.1. Validation of the present simulation

The tube has a diameter of 0.01 m and a length of 0.8 m. The fluid enters the tube with a constant inlet temperature T_{in} of 293 K and with uniform axial velocity V_{in}. The Reynolds number was varied from 10^4 to 10^5. In order to validate the computational model, the numerical results were compared with the theoretical data available for the conventional fluids. The Darcy friction factor given by Blasius is presented as Eq. (20) from White [29].

$$f = 4C_f = 4(0.0791Re^{-1/4}) \tag{20}$$

Fig. 3 displays the comparison of Darcy friction factor from Blasius formula and computed values from the present simulations. An excellent agreement is observed with maximum deviation and average deviation of computed values from theoretical equation being 3.2 and 1.9%, respectively, over the range of Reynolds numbers studied.

Next, the Nusselt number for the fully developed turbulent flow for EG/water is compared with the correlation given by Gnielinski [12].

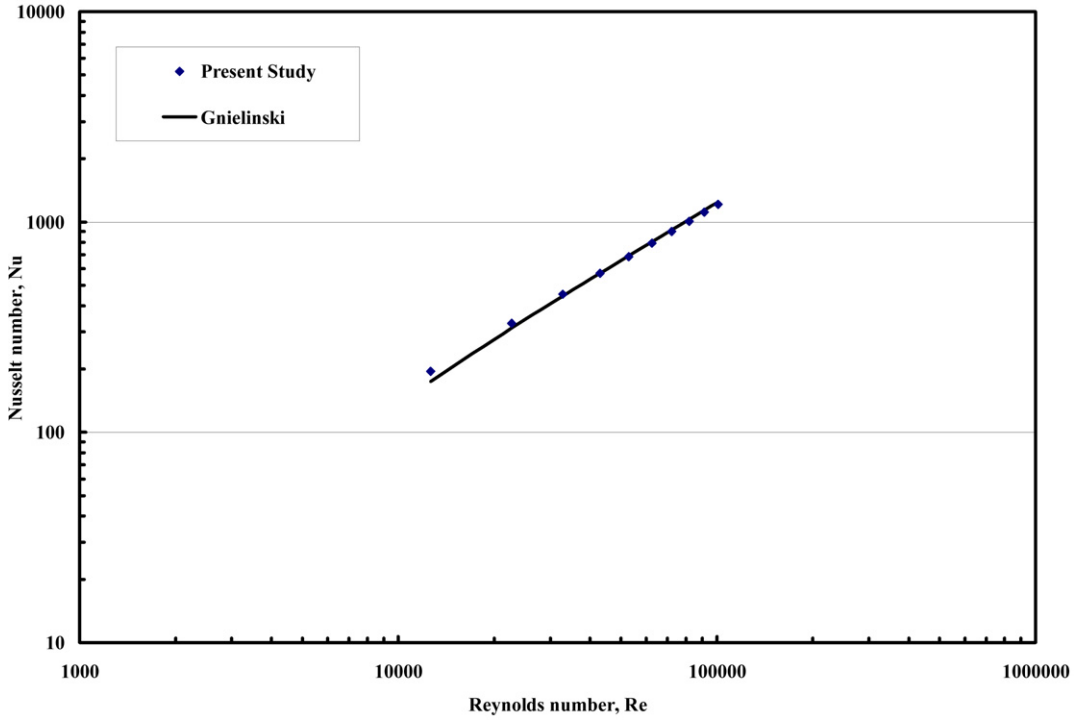

Fig. 4. Comparison between the computed values of Nusselt numbers and the equation given by Gnielinski for EG/water.

Bejan [4] recommends the equation given by Gnielinski, Eq. (21) over the traditional Dittus–Boelter equation, because the errors are usually limited to about ±10%.

$$Nu = 0.012(Re^{0.87} - 280)Pr^{0.4} \quad (21)$$

for $1.5 \leqslant Pr \leqslant 500,\ 3 \times 10^3 \leqslant Re \leqslant 10^6$.

Our simulations were all within this range. Fig. 4 displays comparison of Nusselt numbers obtained from the present numerical analysis for fully developed flow with the equation given by Gnielinski for EG/water. The maximum deviation and average deviation of computed Nusselt number from the equation given by Gnielinski is 10.1 and 5.8%, respectively.

4.2. Application of the model

After the above two comparisons and confirming that the computational model is generating correct results, nanofluids with varying concentrations were analyzed at various Reynolds numbers with applied constant heat flux q'' on the upper wall. A heat flux of 50 W/cm^2 was selected in our simulations because we wanted to compare our results with Maiga et al. [19].

4.2.1. Effect of nanoparticle volume concentration on the Nusselt number

Fig. 5 displays the influence of CuO nanoparticle volume concentration on the Nusselt number. As an example, the increase in the Nusselt number is about 1.35 times with 6% volume concentration of CuO nanoparticles over the base fluid EG/water at Reynolds number of 20000 and the increase in the Nusselt number is about 1.23 times at Reynolds number of 100000. The increase in the Nusselt number is due to the increase in Prandtl number at higher concentrations.

4.2.2. Comparison of computed Nusselt number with other correlations

Fig. 6 displays the comparison of computed Nusselt number from our simulations for a CuO 6% nanofluid with other correlations. As no experimental data is available for CuO 6% nanofluid, we compared our results with the correlation equation (1) by Pak and Cho [24]. Pak and Cho developed the correlation from dilute concentration (0–3%) of Al_2O_3 and TiO_2 nanoparticles in water which have lower Prandtl numbers. The deviation between the present study and the Pak and Cho correlation is due to different nanofluids of higher concentration and higher Prandtl number. Eq. (2) by Maiga et al. [19] predicts higher Nusselt number at lower Reynolds number. This is because they have conducted their numerical computations using constant thermophysical properties evaluated at inlet temperature. However, in reality at lower Reynolds number, the fluid gets heated up and the bulk mean temperature of the fluid increases. This case was observed in our simulations. At higher bulk mean temperature the viscosity value becomes lower. As Prandtl number is directly proportional to viscosity it lowers the Prandtl number, which in turn lowers the Nusselt number which is evident from our simulation. However, at higher Reynolds numbers, the bulk mean temperature of the fluid does not change considerably; this does not affect the viscosity and the Prandtl number and hence there is a closer agreement between Maiga et al. and the present simulation. The computed values of Nusselt number from the present simulation are in good agreement with Eq. (21) developed by Gnielinski [12]. The maximum deviation and average deviation of computed values with equation by Gnielinski were 12 and 6.5%.

A summary of the Prandtl number variation with Reynolds number is compiled in Fig. 7.

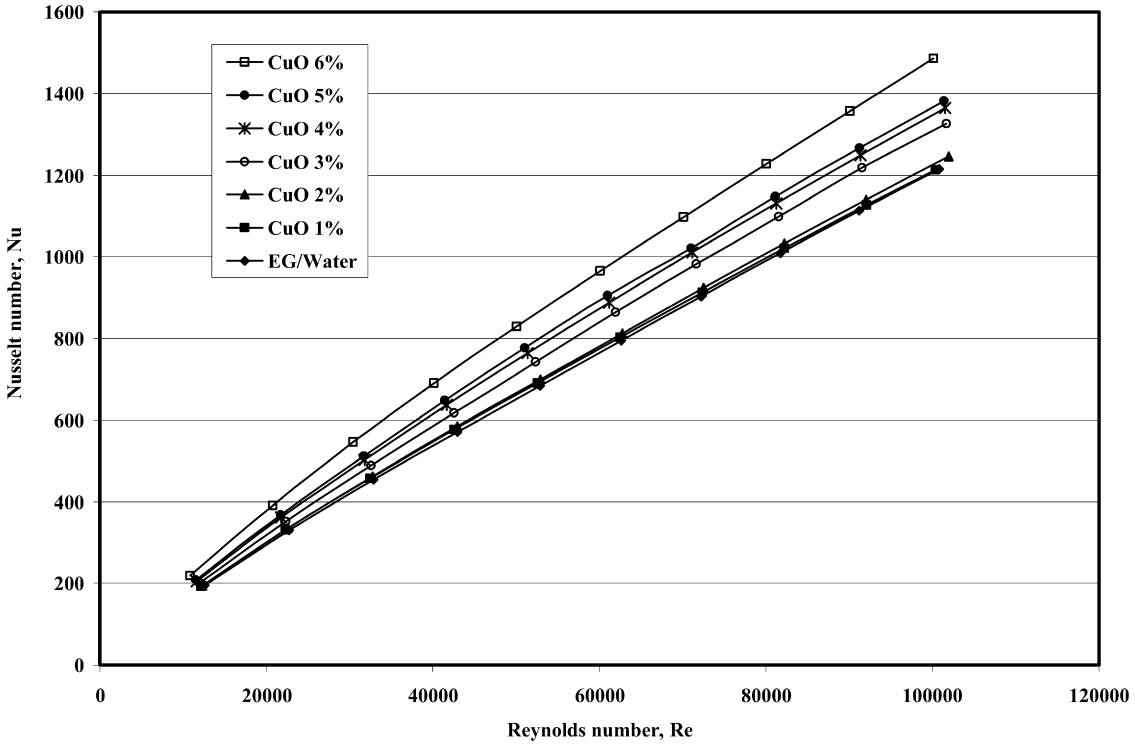

Fig. 5. The influence of copper oxide nanoparticle volume concentration on the Nusselt number over a range of Reynolds numbers.

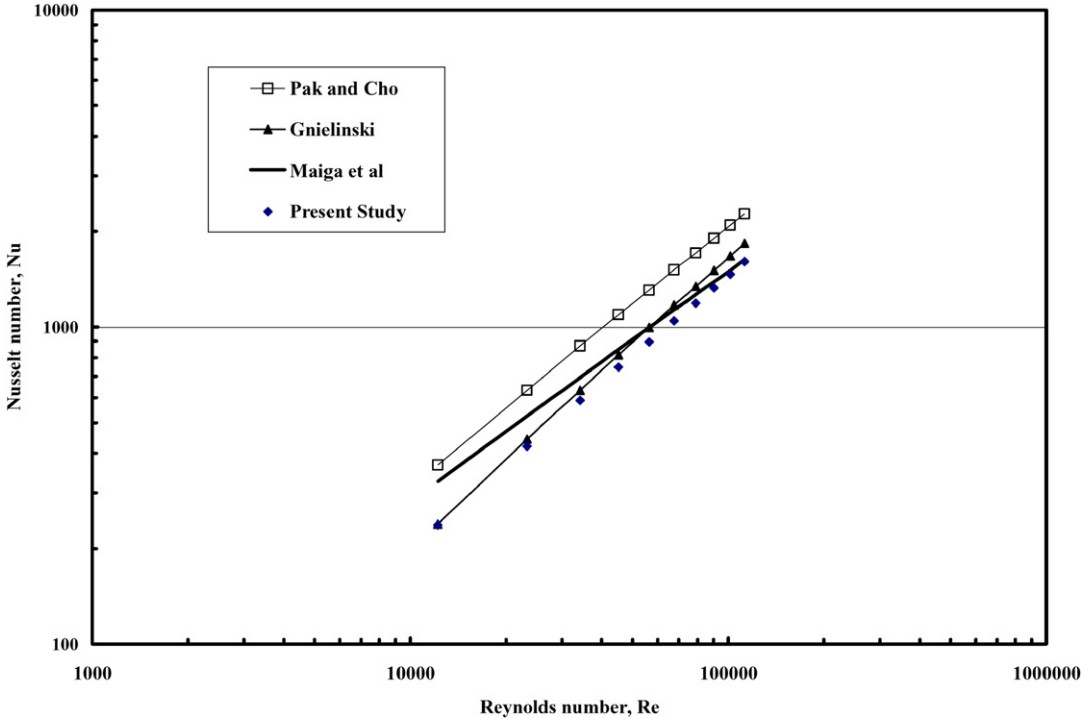

Fig. 6. Comparison of Nusselt number for CuO (6%) with other correlations.

It can be concluded that for all nanofluids of same concentration Prandtl number is low at lower Reynolds numbers and high at higher Reynolds numbers. This is solely due to the bulk mean temperature variation. Similar trend was observed for all concentrations of CuO nanofluids.

4.2.3. Effect of nanoparticle volume concentration on the heat transfer coefficient

Fig. 8 displays the influence of CuO nanoparticle volume concentration on the heat transfer coefficient. For a 6% volume concentration, the increase in heat transfer coefficient

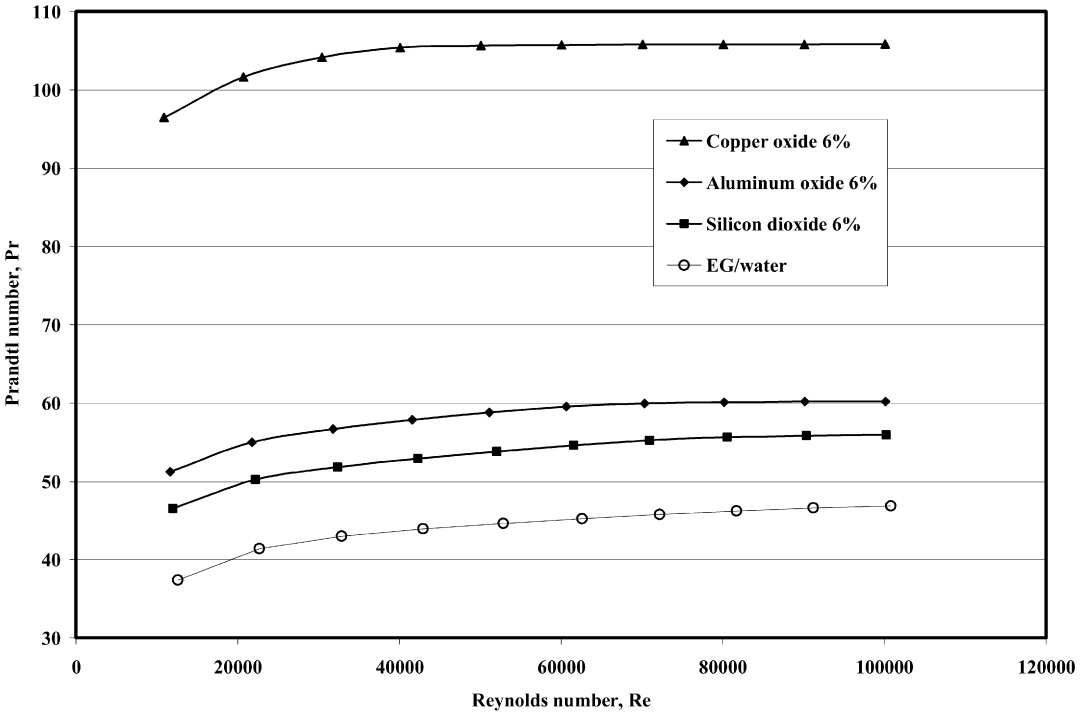

Fig. 7. Variation of Prandtl number with Reynolds number in the present simulations for various nanofluids.

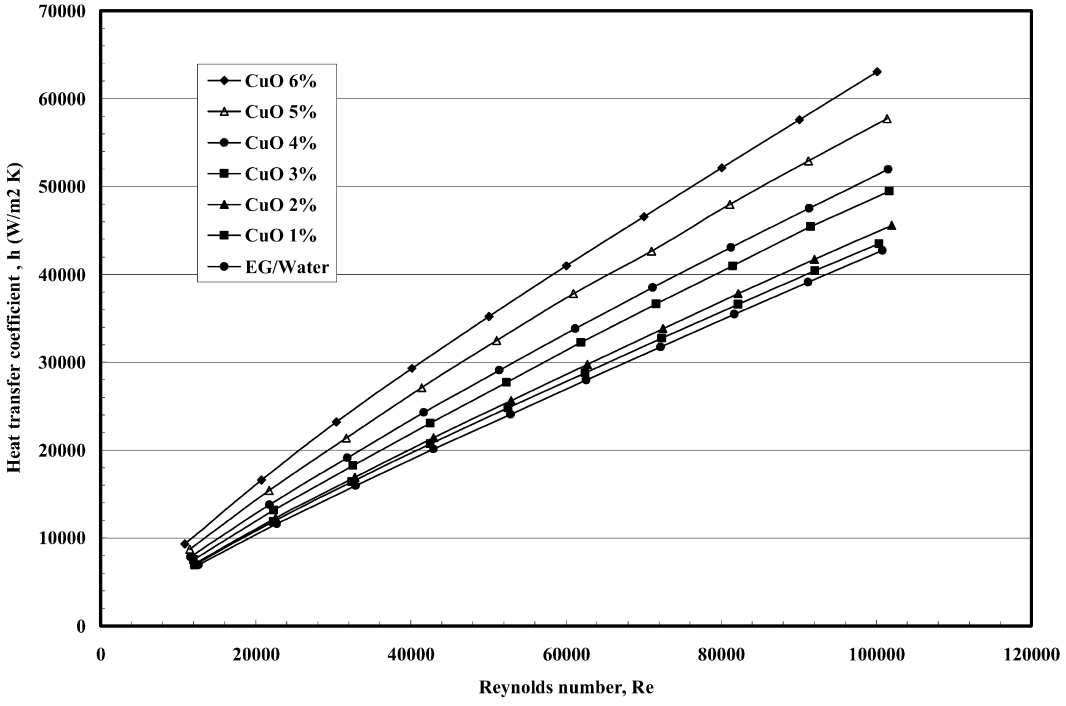

Fig. 8. The influence of copper oxide nanoparticle volume concentration on the heat transfer coefficient over a range of Reynolds numbers.

is about 1.75 times over the base fluid at a Reynolds number of 20000 and is about 1.5 times at Reynolds number of 100000. At lower Reynolds number, the bulk mean temperature is higher making specific heat, thermal conductivity higher and viscosity lower. Therefore a better heat transfer is achieved and hence the relative gain in heat transfer is higher at lower Reynolds number for a fixed concentration.

4.2.4. Comparison between different nanofluids of same volume concentration

Fig. 9 displays the increase in heat transfer coefficient by various nanofluids over the base fluid for a fixed volume concentration of 6%. The increase in heat transfer coefficient is high for CuO nanofluids and is low for SiO_2 nanofluids. This is due to the higher Prandtl number and thermal conductivity of CuO nanofluids than others.

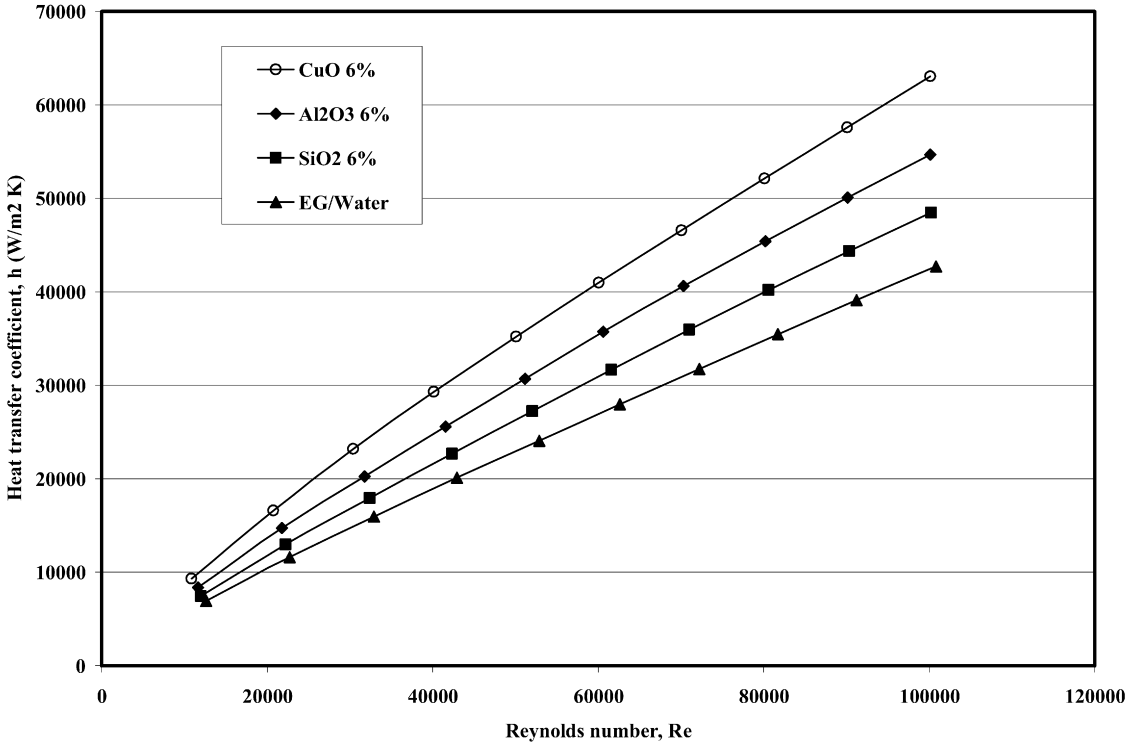

Fig. 9. Comparison of heat transfer coefficient of different nanofluids over the base fluid EG/water.

4.2.5. Effect of nanoparticle diameter on the Nusselt number

Fig. 10 displays the effect of nanoparticle diameter on the Nusselt number for SiO_2 nanofluids of 6% volume concentration. The fluid containing 20 nm particle size have higher Nusselt numbers followed by 50 and 100 nm for same Reynolds number. This is because the viscosity values of 20 nm nanofluid are higher, followed by 50 and 100 nm. Higher the viscosity, higher the Prandtl number for same concentration of SiO_2 nanofluids, not including the particle size effect on thermal conductivity. Future research should concentrate on developing thermal conductivity correlation which takes particle diameter into account. Higher Prandtl number yields higher Nusselt number. Similar enhancement in Nusselt number with lower particle size was observed from the experiments conducted by Nguyen et al. [23]. For the same volume concentration lower diameter particles provide large surface area of interaction with the fluid in exchanging heat.

4.2.6. Effect of nanoparticle volume concentration on the wall shear stress

From Fig. 11, we observe that higher the concentration of the nanofluids, higher is the wall shear stress. Higher the shear stress, higher is the pumping power. Nanofluids with higher volume concentration have higher heat transfer enhancement and also have higher pressure drop. Therefore, judicious decision should be taken when selecting a nanofluid that will balance the heat transfer enhancement and the pressure drop penalty.

Regarding the dependence of fully developed Nusselt number as a function of the flow Reynolds number, Fig. 12 shows the numerical data obtained for three different nanofluids at 6% particle volume concentration and the base fluid. At a Reynolds number of about 60,000 the increase in Nusselt number is about 25% over the base fluid for 6% CuO nanofluid. This enhancement is due to the higher Prandtl number as shown in Fig. 7.

In Fig. 13 a comparison is shown between the numerically computed results and the correlations of Gnielinski and Dittus–Boelter for a 6% concentration of Al_2O_3 nanofluid. In lower range of Reynolds number the agreement of our predicted Nusselt number is very close to the two correlations when compared at higher range of Reynolds number. Even at a Reynolds number of 100000 the deviation in Nusselt number between Gnielinski equation and our computed numerical results is 5.8% and that between Dittus–Boelter and numerical results is 8.6%. Considering the fact that Dittus–Boelter correlation can have a maximum deviation of the order 40% [4] and the formula due to Gnielinski is accurate within $\pm 10\%$, our numerical computations agree quite well with these two correlations. Exactly the same trend was observed for the two other nanofluids at all computed concentrations.

5. Conclusions

Viscosity of nanofluids increases as the particle diameter decreases. New viscosity correlations for nanofluids as a function of volume concentration and temperature were presented. At a fixed Reynolds number of 20000 Nusselt number for 6% CuO nanofluids increases by 1.35 times over the base fluid. At a fixed Reynolds number of 20000 heat transfer coefficient for 6% CuO nanofluids increases by 1.75 times over the base

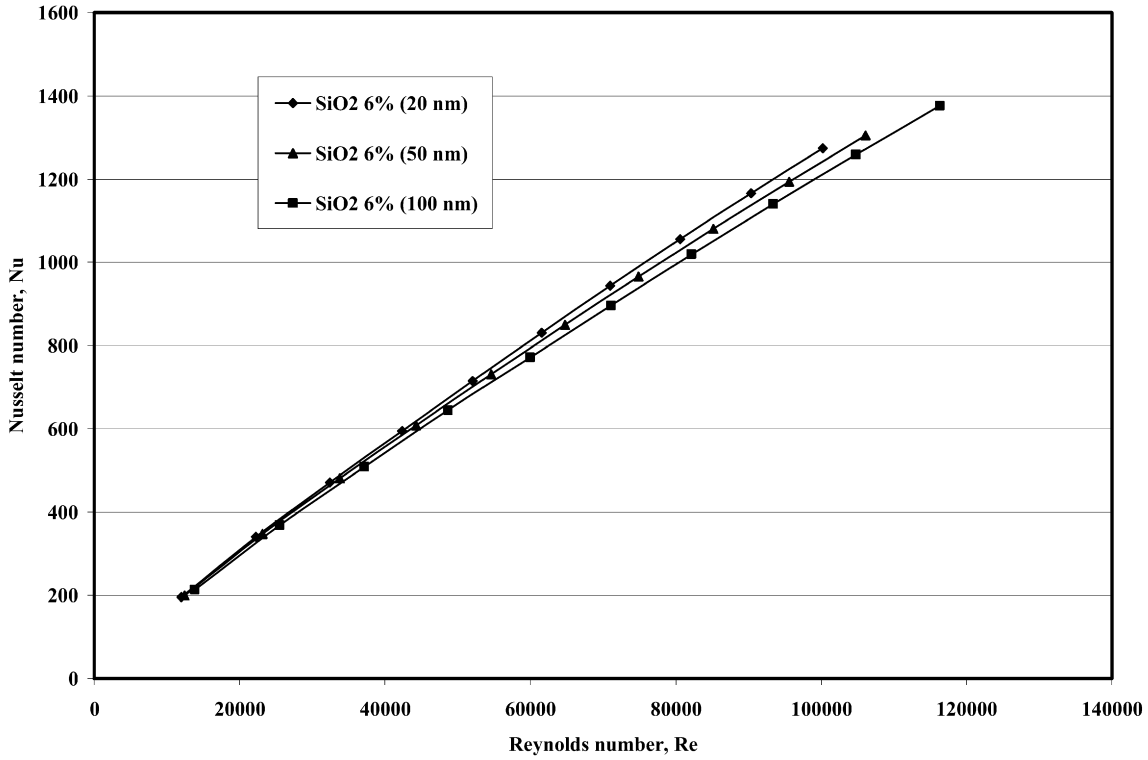

Fig. 10. Effect of nanoparticle diameter on the Nusselt number for a 6% volume concentration of SiO_2 nanofluids.

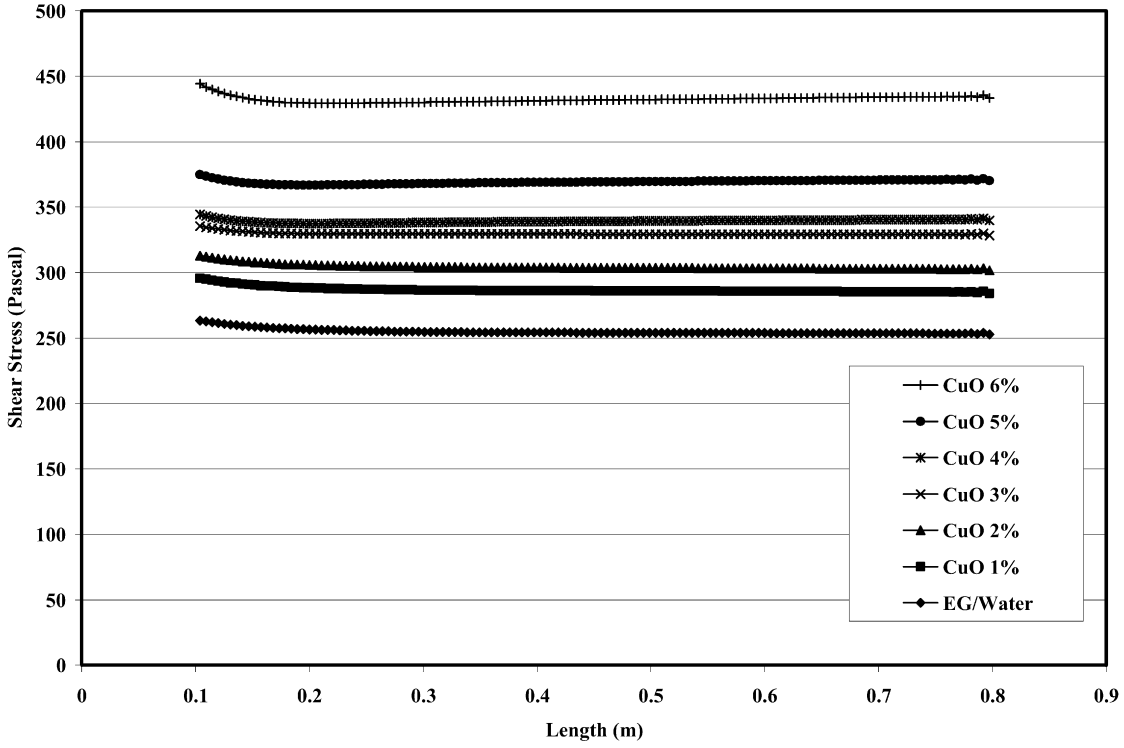

Fig. 11. Effect of nanoparticle volume concentration on the wall shear stress for CuO nanofluids in the fully developed region.

fluid. Heat transfer coefficient of nanofluids increases with increase in the volume concentration of nanofluids and Reynolds number. Higher temperature operation of the nanofluids yields higher percentage increase in heat transfer rate. Prandtl number of nanofluids increases with decrease in the operating temperature, because the viscosity plays a dominant role. For the same concentration of CuO, Al_2O_3 and SiO_2 nanofluids, at a particular Reynolds number, CuO nanofluids have higher heat

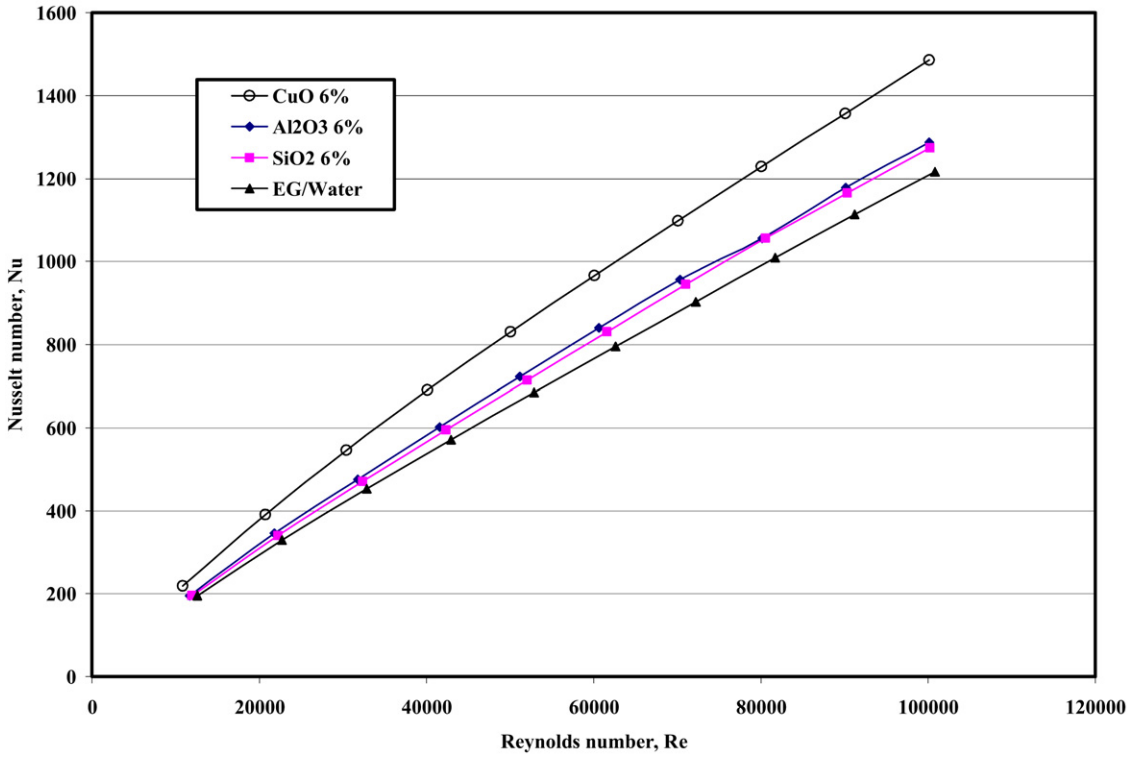

Fig. 12. Comparison of Nusselt number versus Reynolds number for three different nanofluids and the base fluid.

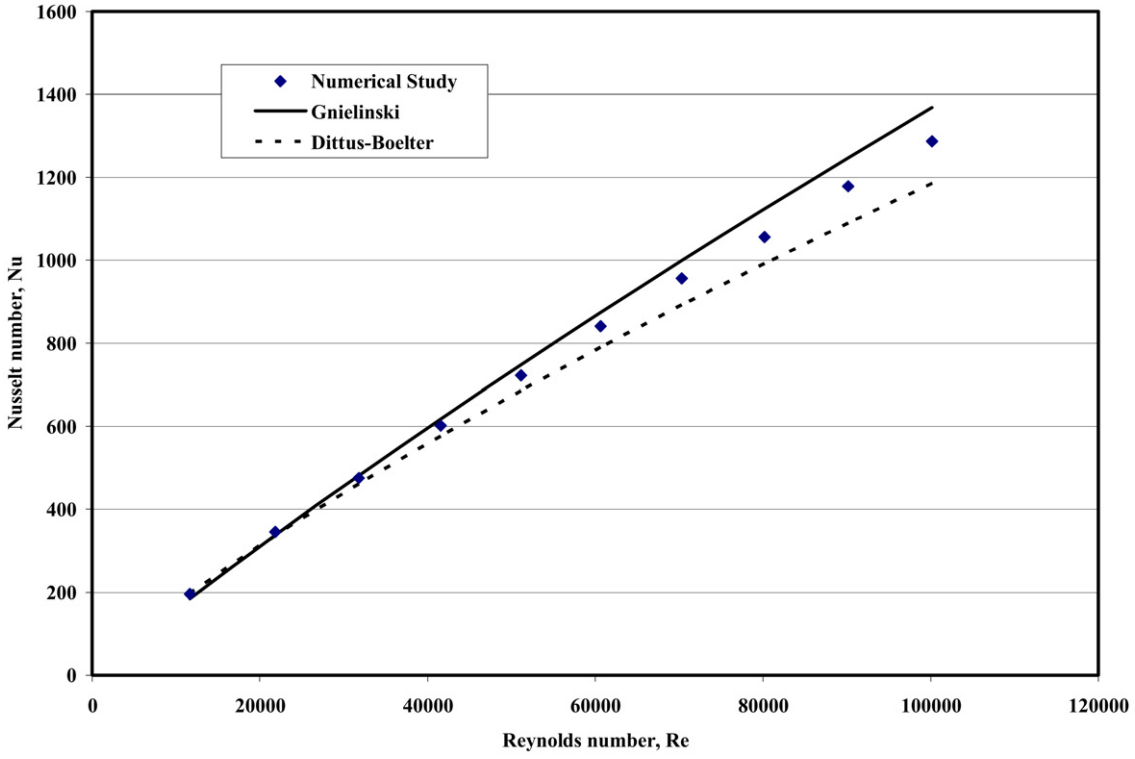

Fig. 13. A comparison of Nusselt number prediction for various Reynolds numbers for 6% Al_2O_3 nanofluid between numerically computed data and Gnielinski and Dittus–Boelter correlations.

transfer performance followed by Al_2O_3 and SiO_2. Pressure loss increases with increase in the volume concentration of the nanofluids. Computed values of the Nusselt numbers are in good agreement with correlation given by Gnielinski. From our analysis we found that Gnielinski correlation can be used in determining the Nusselt number of nanofluids with $47 \leqslant Pr \leqslant 105$ and Reynolds number ranging from $10^4 - 10^5$ with volume concentration up to 6%.

Acknowledgements

Financial assistance from the Arctic Region Supercomputing Center (ARSC) and the Department of Mechanical Engineering at the University of Alaska Fairbanks is gratefully acknowledged.

References

[1] A. Akbarinia, A. Behzadmehr, Numerical study of laminar mixed convection of a nanofluid in horizontal curved tubes, Applied Thermal Engineering 27 (2007) 1327–1337.
[2] ASHRAE Handbook Fundamentals, American Society of Heating, Refrigerating and Air-Conditioning Engineers Inc., Atlanta, 2005.
[3] G.K. Batchelor, The effect of Brownian motion on the bulk stress in a suspension of spherical particles, Journal of Fluid Mechanics 83 (1977) 97–117.
[4] A. Bejan, Heat Transfer, John Wiley & Sons, New Jersey, 1993.
[5] Brookfield Engineering, Brookfield LV DV-II+ Programmable Viscometer Manual No. M/97-164-D1000, Brookfield Engineering Laboratories Inc., Massachusetts, 1999.
[6] J. Buongiorno, Convective transport in nanofluids, Journal of Heat Transfer 128 (2006) 240–250.
[7] S. Choi, Enhancing thermal conductivity of fluids with nanoparticles, ASME Publications 66 (1995) 99–105.
[8] S. Das, N. Putra, P. Thiesen, W. Roetzel, Temperature dependence of thermal conductivity enhancement for nanofluids, Journal of Heat Transfer 125 (2003) 567–574.
[9] F.W. Dittus, L.M.K. Boelter, Heat transfer for automobile radiators of the tubular type, University of California Publications in Engineering 2 (1930) 443.
[10] J.A. Eastman, S.U.S. Choi, S. Li, W. Yu, L.J. Thompson, Anomalously increased effective thermal conductivities of ethylene glycol-based nanofluids containing copper nanoparticles, Applied Physics Letters 78 (2001) 718–720.
[11] Fluent 6.2 user guide, Fluent Inc., Lebanon, New Hampshire, 2005.
[12] V. Gnielinski, New equations for heat and mass transfer in turbulent pipe and channel flow, International Chemical Engineering 16 (1976) 359–367.
[13] R.L. Hamilton, O.K. Crosser, Thermal conductivity of heterogeneous two-component system, I and EC Fundamentals 1 (1962) 187–191.
[14] S.Z. Heris, M.N. Esfahany, G. Etemad, Investigation of CuO/water nanofluid laminar convective heat transfer through a circular tube, Journal of Enhanced Heat Transfer 13 (2006) 279–289.
[15] D.P. Kulkarni, D.K. Das, G.A. Chukwu, Temperature dependent rheological property of copper oxide nanoparticles suspension (nanofluid), Journal of Nanoscience and Nanotechnology 6 (4) (2006) 1150–1154.
[16] D.P. Kulkarni, D.K. Das, S.L. Patil, Effect of temperature on rheological properties of copper oxide nanoparticles dispersed in propylene glycol and water mixture, Journal of Nanoscience and Nanotechnology 7 (6) (2007) 1–5.
[17] B.E. Launder, D.B. Spalding, Mathematical Models of Turbulence, Academic Press, New York, 1972.
[18] S.B. Maiga, S.J. Palm, C.T. Nguyen, G. Roy, N. Galanis, Heat transfer enhancement by using nanofluids in forced convection flows, International Journal of Heat and Fluid Flow 26 (2005) 530–546.
[19] S.B. Maiga, C.T. Nguyen, N. Galanis, G. Roy, T. Mare, M. Coqueux, Heat transfer enhancement in turbulent tube flow using Al_2O_3 nanoparticle suspension, International Journal of Numerical Methods for Heat and Fluid Flow 16 (2006) 275–292.
[20] F.C. McQuiston, J.D. Parker, J.D. Spitler, Heating Ventilating and Air Conditioning, John Wiley & Sons Inc., New York, 2000.
[21] P.K. Namburu, D.P. Kulkarni, D. Misra, D.K. Das, Viscosity of copper oxide nanoparticles dispersed in ethylene glycol and water mixture, Experimental Thermal and Fluid Science 32 (2007) 397–402.
[22] P.K. Namburu, D.P. Kulkarni, A. Dandekar, D.K. Das, Experimental investigation of viscosity and specific heat of silicon dioxide nanofluids, Micro & Nano Letters 2 (3) (2007) 67–71.
[23] C.T. Nguyen, G. Roy, C. Gauthier, N. Galanis, Heat transfer enhancement using Al_2O_3–water nanofluid for an electronic liquid cooling system, Applied Thermal Engineering 27 (2007) 1501–1506.
[24] B.C. Pak, Y.I. Cho, Hydrodynamic and heat transfer study of dispersed fluids with submicron metallic oxide particles, Experimental Heat Transfer 11 (1998) 151–170.
[25] S.V. Patankar, Numerical Heat Transfer and Fluid Flow, Hemisphere Publishing Corporation, New York, 1980.
[26] T.M. Shih, Numerical Heat Transfer, Hemisphere Publishing Corporation, New York, 1984.
[27] Y. Xuan, Q. Li, Investigation on convective heat transfer and flow features of nanofluids, Journal of Heat Transfer 125 (2003) 151–155.
[28] X.Q. Wang, A.S. Mujumdar, Heat transfer characteristics of nanofluids: a review, International Journal of Thermal Sciences 46 (2007) 1–19.
[29] F.M. White, Viscous Fluid Flow, McGraw Hill, New York, 1991.
[30] X. Zhang, H. Gu, M. Fujii, Effective thermal conductivity and thermal diffusivity of nanofluids containing spherical and cylindrical nanoparticles, Journal of Applied Physics 100 (4) (2006) 044325, 1–5.